

Hunting for wandering massive black holes with ngVLA

Kohei Inayoshi¹, Tomonari Michiyama¹

¹*Kavli Institute for Astronomy and Astrophysics, Peking University, Beijing 100871, People's Republic of China*
inayoshi@pku.edu.cn

Abstract

Supermassive black holes (SMBHs) are almost ubiquitously harbored in the nuclei of massive galaxies, which were assembled through galaxy mergers. As a natural outcome of frequent mergers, wandering massive BHs are likely to be populated via ejection from the galactic nuclei through multi-body BH interactions and gravitational wave recoils. Those wandering BHs are expected to plunge into diffuse and hot plasma (with an electron density of $\simeq 0.1 \text{ cm}^{-3}$ and temperature of $\simeq 10^7 \text{ K}$) and be fed with the gas at a rate of $\simeq 10^{-7} - 10^{-6} \dot{M}_{\text{Edd}}$, where \dot{M}_{Edd} is the Eddington accretion rate. Radiation spectra from such radiatively inefficient accretion flows onto the wandering BH have a peak at the millimeter band, where the next-generation Very Large Array (ngVLA) has the highest sensitivity. Therefore, future observations with ngVLA will enable us to hunt wandering BH population and push the detection limit of wandering BH's masses down to $M_{\bullet} \simeq 5 \times 10^6 M_{\odot}$ for massive nearby ellipticals, e.g., M87, and $M_{\bullet} \simeq 3 \times 10^4 M_{\odot}$ for Milky Way. With the capability of ngVLA, additional 8 nearby elliptical galaxies are interesting targets for hunting wandering BHs, assuming that those BHs are as massive as $\gtrsim 1\%$ of the nuclear SMBHs. The detection of wandering BHs is a key missing piece to understand the entire BH population and give physical interpretations of off-nuclear BHs detected in dwarf galaxies, which may constrain BH seed formation scenarios.

Key words: Accretion (14); Gravitational waves (678); Interstellar medium (847); Radio continuum emission (1340); Supermassive black holes (1663)

1. Introduction

Galaxies were assembled out of smaller mass via halo and galaxy mergers in the framework of hierarchical structure formation. As a natural result of frequent galaxy mergers, incoming massive BHs would sink toward the centers, form binary SMBHs at the galactic nuclei, and coalesce with gravitational wave (GW) emission, if the BHs would successfully decay their orbit via dynamical processes within a Hubble time (Begelman et al. 1980; Yu 2002; Merritt 2013; Khan et al. 2016; Kelley et al. 2017). The GW emission associated with their mergers will provide useful insights for us to understand the population of massive binary BHs with future space-based GW observatories (LISA, Tianqin, Taiji) and pulsar-timing-array experiments (PTAs) (Sesana et al. 2008; Inayoshi et al. 2018a; Bonetti et al. 2018a; Luo et al. 2016)

In giant ellipticals, which are the most massive objects in the local universe and have experienced a large number of minor and dry mergers at low redshifts. In gas-poor environments, multiple BH encounters in the nuclei would be likely to make the most massive two BHs coalesce but simultaneously to eject less massive ones from the nuclei (Bonetti et al. 2018a; Ryu et al. 2018). Similarly, merger remnants due to the successive BH interactions would be kicked by the anisotropic emission of GWs (or ‘gravitational recoil’) during the final BH coalescences (Bekenstein 1973; Campanelli 2005; Lousto et al. 2012). Those ejected BHs with a mass range of $M_{\bullet} \simeq 10^6 - 10^8 M_{\odot}$ at high velocities comparable to the escape speed from the galactic cores are expected to orbit at the outskirts of galaxies as “wandering BHs”.

Wandering BHs would also be important candidates of

intermediate-mass BHs (IMBHs). In the Milky-Way galaxy and low-mass dwarf galaxies, the existence of IMBHs (see a recent review by Greene et al. 2020) with $M_{\bullet} \gtrsim 10^4 M_{\odot}$ has been argued based on observations of high-velocity compact clouds in the Galactic center (Oka et al. 2017) and off-nuclear compact radio sources in dwarf galaxies (Reines et al. 2020). Numerical simulations also predict that Milky Way-size halos would host ~ 10 IMBHs within their virial radii, and that they would wandering within their host galaxies for several Gyr (Bellovary et al. 2010; Tremmel et al. 2018a). The detection of IMBHs is a key missing piece to understand the entire BH population (from stellar-mass to super-massive regimes) and the properties of wandering BHs may constrain their seeding mechanisms (see a recent review by Inayoshi et al. 2020).

2. Radiation properties of wandering and accreting BHs

Wandering BHs in the outskirts of galaxies are likely to be embedded in hot and diffuse plasma with density of $n_e \simeq 0.1 \text{ cm}^{-3}$ and temperature of $T \simeq 10^7 \text{ K}$ (Russell et al. 2013) and to be fed with the matter. Adopting the typical properties of the plasma, the canonical Bondi-Hoyle-Littleton (BHL) mass accretion rate onto a moving BH with a mass of M_{\bullet} at a speed of v_{∞} is given by

$$\dot{M}_{\text{BHL}} = \frac{4\pi G^2 M_{\bullet}^2 \rho_{\infty}}{c_{\infty}^3 (1 + \mathcal{M}^2)^{3/2}}. \quad (1)$$

(Hoyle & Lyttleton 1939; Bondi 1952), where $\mathcal{M} \equiv v_{\infty}/c_{\infty}$ is the Mach number, ρ_{∞} and c_{∞} are the density and sound speed of plasma. The accretion rate normalized by the Eddington rate is given by

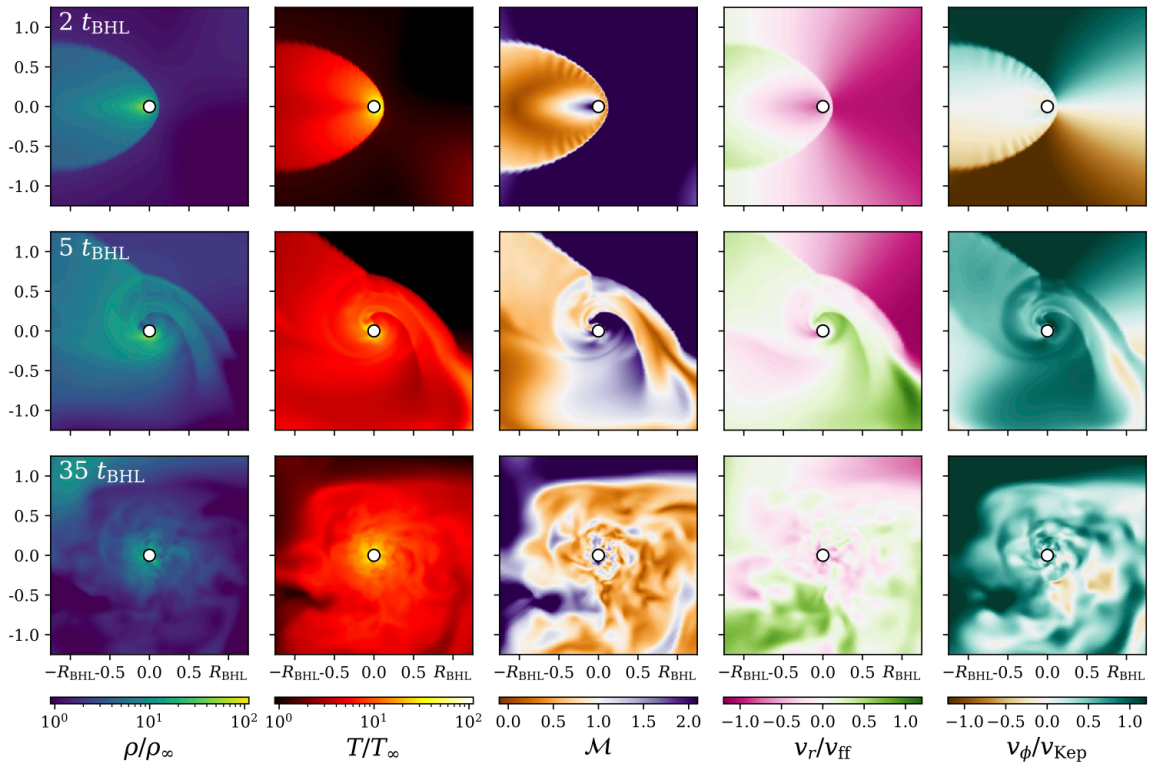


Fig. 1. Snapshots of accretion flows onto a moving BH at three different elapsed times. From the left to the right, we show the gas density, temperature, Mach number, radial velocity normalized by free-fall velocity, and azimuthal velocity normalized by the Keplerian velocity. The accretion flow is symmetric with respect in the early stage (top panels), forms a spiral structure owing to angular momentum supply (middle panels), and becomes highly turbulent in the late stage (bottom panels). As a result of turbulence, the BH feeding rate is limited to $\sim 10 - 20\%$ of the BHL rate, which corresponds to $\dot{m}_{\text{BHL}} \sim O(10^{-7})$.

$$\dot{m}_{\text{BHL}} \simeq 1.5 \times 10^{-6} (1 + \mathcal{M}^2)^{-3/2} \times \left(\frac{M_{\bullet}}{10^7 M_{\odot}} \right) \left(\frac{n_e}{0.1 \text{ cm}^{-3}} \right) \left(\frac{T}{10^7 \text{ K}} \right). \quad (2)$$

At such low rates, the accreting matter does not cool but forms a geometrically thick and hot disk; the so-called radiatively inefficient accretion flows (RIAFs) (Ichimaru 1977; Narayan & Yi 1994; Narayan & Yi 1995a; Narayan et al. 2000; Quataert & Gruzinov 2000; Blandford & Begelman 2004; Yuan & Narayan 2014).

Recently, Guo et al. (2020) studied the dynamics of accretion flows onto a wandering BH at such a low accretion rate (RIAF regime), performing three-dimensional hydrodynamical simulations (see Fig. 1). They found that a wandering BH is fed with hot and diffuse plasma, and the accretion flow becomes turbulent. In the turbulent medium with a wide distribution of inflowing angular momentum, the mass accretion rate is limited at $\sim 10 - 20\%$ of the canonical BHL rate; namely, the BH feeding rate corresponds to $\dot{m}_{\text{BHL}} \simeq O(10^{-7})$ for $M_{\bullet} \simeq 10^7 M_{\odot}$. From the analogy of low-luminosity SMBHs in the nearby universe, e.g., Sagittarius A*, most of the radiation energy is released in the radio band (e.g., Yuan et al. 2004), where the next generation VLA (ngVLA) has the highest sensitivity and spatial resolution. Therefore, ngVLA will be a powerful tool to hunt for a population of wandering BHs.

3. Detectability of wandering BHs

In this section, we calculate the radiation spectral energy distribution (SED) of accretion flows onto a moving BH and discuss the detectability of wandering BHs in different types of galaxies. Here, the mass accretion rate through the nuclear accretion disk, where most radiation is generated, is calculated from the hydrodynamical simulations, and the radiation spectra from the RIAF is obtained with a semi-analytical two-temperature disk model (Manmoto et al. 1997; Yuan et al. 2004). In the following, we consider the radiation spectra from wandering BHs that accrete gas at the outskirts of elliptical galaxies, the Milky Way, and dwarf galaxies and discuss their detectability by ngVLA.

3.1. Elliptical galaxies

First, as an example of a massive elliptical galaxy, we consider M87. Based on the *Chandra* observational data from Russell et al. (2015), the properties of gas surrounding a wandering BH are given; the electron density $n_e \simeq 0.11 \text{ cm}^{-3}$ and temperature $T \simeq 1.9 \times 10^7 \text{ K}$ at a distance of $r \simeq 2 - 3 \text{ kpc}$ from the center. Here, the mass of the wandering BH is set to $M_{\bullet} \simeq 10^{7-8} M_{\odot}$ (Zivancev et al. 2020), which corresponds to $\simeq 0.1 - 1\%$ of the mass of the central SMBH ($\simeq 6 \times 10^9 M_{\odot}$; Event Horizon Telescope Collaboration et al. 2019), and the orbital velocity of the wandering BH is assumed to be $\sim c_s$,

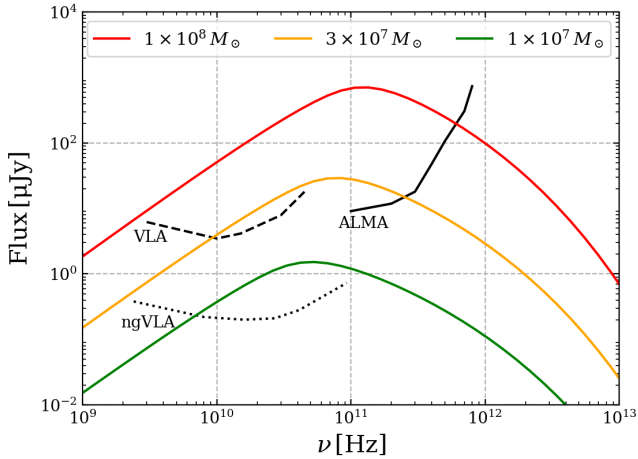


Fig. 2. Radiation spectra from a wandering BH that accretes hot and diffuse plasma in the outskirts of the massive elliptical M87 galaxy. Each curve corresponds to the case with different BH mass ($10^7 \leq M_{\bullet}/M_{\odot} \leq 10^8$). The black curves show the ngVLA sensitivity to continuum emission for 1 hour on-source integration (<https://ngvla.nrao.edu/page/performance>), and the continuum sensitivity curves of VLA and ALMA under the same conditions. Wandering BHs with masses of $M_{\bullet} \gtrsim 5 \times 10^6 M_{\odot}$, if any, could be detectable with ngVLA.

i.e., $\mathcal{M} \simeq 1$.

Fig. 2 presents the radiation spectra with different BH masses of $M_{\bullet} = 10^7, 3 \times 10^7, \text{ and } 10^8 M_{\odot}$. We also overlay the sensitivity curve of ngVLA, VLA, and ALMA. For all the cases, the radiation spectra have peaks in the millimeter band at $\nu_p \simeq 50 - 100$ GHz. With the ongoing facilities such as VLA and ALMA, only heavy wandering BHs ($> 3 \times 10^7 M_{\odot}$) could be detectable. As the peak frequency is lowered for lower-mass BHs, the emission from a wandering BHs with $\lesssim 10^7 M_{\odot}$ would peak in the band where ngVLA has the highest sensitivity. Within the design sensitivity curve of ngVLA, the detection limit of wandering BH's masses would be reduced down to $\simeq 5 \times 10^6 M_{\odot}$. Those less-massive BHs would be more likely to be wandering BH populations according to BH ejection through multi-body interactions in the galactic center (Zivancev et al. 2020).

We apply this argument to other nearby massive elliptical galaxies, assuming the existence of wandering BHs at their galaxy outskirts (listed in Table 1). Taking the observational data (Russell et al. 2013; Russell et al. 2015; Inayoshi et al. 2020), we estimate the properties of gas surrounding those BHs and calculate the radiation spectra shown in Fig. 3. The errors of density and temperature are given by the maximum and minimum values at distances of $r \simeq 2 - 3$ kpc from the centers. We assume the mass of the wandering BH to be 1% of the central SMBH mass, and we choose $\mathcal{M} = 0.5$. As shown in Fig. 3 and Table 1, the radio fluxes at $\nu = 50$ Hz are the orders of $10^{-1.5} - 10^2 \mu\text{Jy}$. With the capability of ngVLA, therefore, BHs, if any, wandering at the galactic outskirts could be detectable in 8 nearby elliptical galaxies in addition to M87. In future, more detections of those wandering BHs in nearby ellipticals will enable us to reveal the statistical properties of those populations and to study the nature of BH merger events

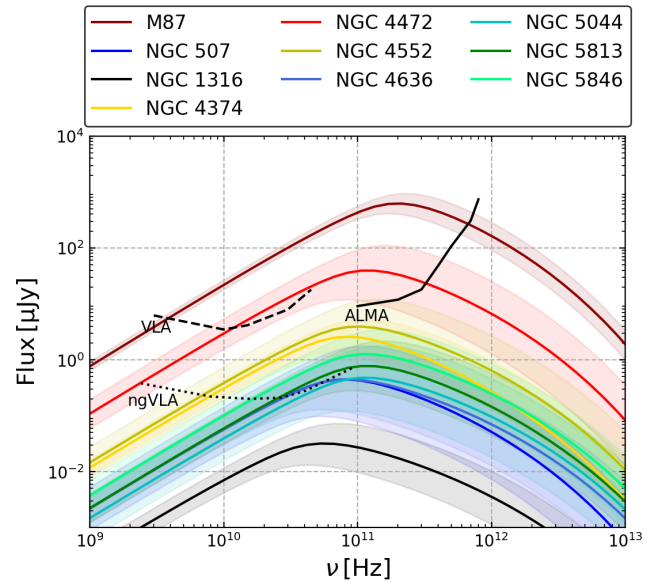


Fig. 3. Radiation spectra from a wandering BH in several different local elliptical galaxies listed in Table 1. The mass of the wandering BH is assumed to be 1% of the central SMBH mass. With the capability of ngVLA, therefore, BHs, if any, wandering at the galactic outskirts could be detectable in 8 nearby elliptical galaxies in addition to M87.

associated with galaxy coalescences.

3.2. Milky Way and dwarf galaxies

Next, we consider the same exercise as in §3.1 for wandering BHs with kpc-scale orbits within the Milky Way. To model the properties of the hot gas surrounding the Milky Way halo, we adopt the results of the Suzaku X-ray observations (Nakashima et al. 2018), which estimate a plasma temperature of $T \simeq 3 \times 10^6$ K and an emission measure of $\text{EM} \simeq (0.6 - 16.4) \times 10^{-3} \text{ cm}^{-6} \text{ pc}$. Based on these results, we adopt $n_e = 0.01 \text{ cm}^{-3}$ as the gas density around wandering BHs. In Fig. 4, we show the radiation spectra of wandering BHs with $M_{\bullet} \simeq 3 \times 10^4 - 3 \times 10^5 M_{\odot}$ located at ~ 10 kpc from the Earth. The spectra in the millimeter band extend to lower frequencies, where (ng)VLA has the highest sensitivity. We could detect IMBHs down to $M_{\bullet} \gtrsim 3 \times 10^4 M_{\odot}$.

Recent radio observations of dwarf galaxies with the VLA by Reines et al. (2020) reported a sample of wandering IMBH candidates that are significantly offset from the optical centers of the host galaxies. Based on an empirical scaling relation between BH mass and total stellar mass, the authors argued that the candidate wandering BHs might have masses in the range $M_{\bullet} \simeq 10^4 - 10^6 M_{\odot}$. The measurements of multi-band radio spectra for those wandering BH candidates by a higher sensitivity of ngVLA will allow us to study the radiation mechanism and reveal the origin of the emission. In future, more detections of wandering BHs in dwarf galaxies would constrain BH seed formation scenarios.

References

Begelman, M. C., Blandford, R. D., & Rees, M. J. 1980, *Nature*, 287, 307

Name (1)	D (Mpc) (2)	$\log(M_{\bullet}/M_{\odot})$ (3)	n_e (cm $^{-3}$) (4)	T (keV) (5)	$\log \dot{m}$ (6)	$\log(F_{\nu_p}/\mu\text{Jy})$ (7)
M87	16.68	9.789 ± 0.027	0.114 ± 0.016	1.650 ± 0.050	-5.918 ± 0.104	1.992 ± 0.096
NGC 4472	16.72	9.400 ± 0.100	0.029 ± 0.010	0.785 ± 0.005	-6.418 ± 0.233	1.065 ± 0.297
NGC 4552	15.30	8.920 ± 0.110	0.018 ± 0.004	0.455 ± 0.035	-6.738 ± 0.257	0.146 ± 0.339
NGC 4374	18.51	8.970 ± 0.050	0.022 ± 0.005	0.595 ± 0.025	-6.778 ± 0.157	0.021 ± 0.202
NGC 5846	24.90	8.820 ± 0.110	0.042 ± 0.009	0.625 ± 0.015	-6.689 ± 0.210	-0.407 ± 0.304
NGC 5813	32.20	8.810 ± 0.110	0.042 ± 0.009	0.585 ± 0.015	-6.661 ± 0.208	-0.633 ± 0.304
NGC 507	70.80	9.210 ± 0.160	0.029 ± 0.009	0.965 ± 0.015	-6.742 ± 0.288	-0.726 ± 0.465
NGC 4636	14.70	8.490 ± 0.080	0.028 ± 0.011	0.485 ± 0.015	-7.029 ± 0.244	-0.731 ± 0.304
NGC 5044	31.20	8.710 ± 0.170	0.050 ± 0.009	0.645 ± 0.015	-6.748 ± 0.254	-0.822 ± 0.431
NGC 1316	20.95	8.230 ± 0.080	0.033 ± 0.007	0.620 ± 0.010	-7.385 ± 0.181	-1.803 ± 0.325

Table 1. Column 1: galaxy name; Column 2: distance; Column 3: mass of the central BH; Column 4 and 5: electron density and temperature at $\sim 2 - 3$ kpc; Column 6: accretion rate normalized by the Eddington rate ($\dot{m} \equiv \dot{M}/\dot{M}_{\text{Edd}}$) by the scaling relation from the simulation A1, assuming the wandering BH mass is 1% of the central BH mass and $\mathcal{M} = 0.5$; Column 7: radiation flux density at $\nu_p = 50$ GHz, where the ngVLA sensitivity flux is $\simeq 0.3 \mu\text{Jy}$. The distance and central BH mass are taken from Inayoshi et al. (2020). The electron density and temperature are taken from Russell et al. (2015) for M87 galaxy and from Russell et al. (2013) for the others.

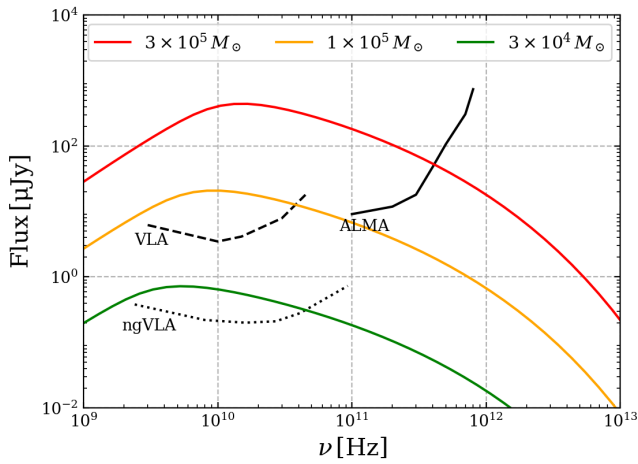


Fig. 4. Radiation spectra from BHs wandering in the outskirts of the Milky Way. Each curve corresponds to the case with different BH mass of $3 \times 10^4 \leq M_{\bullet}/M_{\odot} \leq 3 \times 10^5$.

Bekenstein, J. D. 1973, *ApJ*, 183, 657
Bellovary, J. M., Governato, F., Quinn, T. R., et al. 2010, *ApJL*, 721, L148
—, 2004, *MNRAS*, 349, 68
Bondi, H. 1952, *MNRAS*, 112, 195
Bonetti, M., Haardt, F., Sesana, A., & Barausse, E. 2018a, *MNRAS*, 477, 3910
Campanelli, M. 2005, *Classical and Quantum Gravity*, 22, S387
Event Horizon Telescope Collaboration, Akiyama, K., Alberdi, A., et al. 2019, *ApJ*, 875, L1
Guo, M., Inayoshi, K., Michiyama, T., et al. 2020, *ApJ*, 901, 39
Greene, J. E., Strader, J., & Ho, L. C. 2020, *ARA&A* in press, arXiv:1911.09678
Hoyle, F., & Lyttleton, R. A. 1939, *Proceedings of the Cambridge Philosophical Society*, 35, 405
Ichimaru, S. 1977, *ApJ*, 214, 840
Inayoshi, K., Ichikawa, K., & Haiman, Z. 2018a, *ApJL*, 863, L36
Inayoshi, K., Ichikawa, K., & Ho, L. C. 2020, *ApJ*, 894, 141
Inayoshi, K., Ostriker, J. P., Haiman, Z., & Kuiper, R. 2018b, *MNRAS*, 476, 1412
Inayoshi, K., Visbal, E., & Haiman, Z. 2020, *ARA&A*, 58, 27
Kelley, L. Z., Blecha, L., & Hernquist, L. 2017, *MNRAS*, 464, 3131

Khan, S., Husa, S., Hannam, M., et al. 2016, *Phys. Rev. D*, 93, 044007
Lousto, C. O., Zlochower, Y., Dotti, M., & Volonteri, M. 2012, *Phys. Rev. D*, 85, 084015
Luo, J., Chen, L.-S., Duan, H.-Z., et al. 2016, *Classical and Quantum Gravity*, 33, 035010
Mamato, T., Mineshige, S., & Kusunose, M. 1997, *ApJ*, 489, 791
Merritt, D. 2013, *Classical and Quantum Gravity*, 30, 244005
Nakashima, S., Inoue, Y., Yamasaki, N., et al. 2018, *ApJ*, 862, 34
Narayan, R., Igumenshchev, I. V., & Abramowicz, M. A. 2000, *ApJ*, 539, 798
Narayan, R., & Yi, I. 1994, *ApJL*, 428, L13
—, 1995a, *ApJ*, 444, 231
Oka, T., Tsujimoto, S., Iwata, Y., Nomura, M., & Takekawa, S. 2017, *Nature Astronomy*, 1, 709
Quataert, E., & Gruzinov, A. 2000, *ApJ*, 539, 809
Reines, A. E., Condon, J. J., Darling, J., & Greene, J. E. 2020, *ApJ*, 888, 36
Russell, H. R., Fabian, A. C., McNamara, B. R., & Broderick, A. E. 2015, *MNRAS*, 451, 588
Russell, H. R., McNamara, B. R., Edge, A. C., et al. 2013, *MNRAS*, 432, 530
Ryan, B. R., Ressler, S. M., Dolence, J. C., et al. 2017, *ApJL*, 844, L24
Ryu, T., Perna, R., Haiman, Z., Ostriker, J. P., & Stone, N. C. 2018, *MNRAS*, 473, 3410
Sesana, A., Vecchio, A., & Colacino, C. N. 2008, *MNRAS*, 390, 192
Tremmel, M., Governato, F., Volonteri, M., Pontzen, A., & Quinn, T. R. 2018a, *ApJL*, 857, L22
Yu, Q. 2002, *MNRAS*, 331, 935
Yuan, F., & Narayan, R. 2014, *ARA&A*, 52, 529
Yuan, F., Quataert, E., & Narayan, R. 2004, *ApJ*, 606, 894
Zivacev, C., Ostriker, J., & Kupper, A. H. W. 2020, *MNRAS*, 498, 3807